JOURNAL OF MATERIALS SCIENCE 28 (1993) 6418–6426

Superconducting properties of $YBa_2Cu_3O_7$–Au composites

C. NGUYEN VAN HUONG, M. NICOLAS, A. DUBON, C. HINNEN*
Laboratoire de Physique du Solide, ESPCI, 10 rue Vauquelin, 75231 Paris cedex 05, France

By X-ray diffraction and photoelectron spectroscopy, we have demonstrated that Au is incorporated in the YBCO lattice up to a concentration 0.1. An XPS study gave evidence for an electronic valence state Au^{1+}. Its replacement in the Cu(1) site appears questionable due to the large difference in ionic radii (Cu^{2+}: 0.073 nm; Au^{1+}: 0.137 nm). The so called 'irreversibility lines' determined by AC susceptibility measurements are strongly affected by the doping. Up to the limit of solubility in the grains, an improvement in intra and intergrain coupling and flux pinning energy is observed, showing the beneficial interest of YBCO–Au composites.

1. Introduction

Chemical doping of high T_c superconductors by additives or substituents has been widely investigated. The substitution at barium or copper sites induces a degradation of T_c [1]. Despite the similarity of the valence electron structure of Ag and Au with Cu, noble metals substitute very little for Cu in $YBa_2Cu_3O_7$ [2, 3]. However, when they are included as additives to stoichiometric YBCO during synthesis, YBCO–Ag or YBCO–Au composites are obtained. YBCO–Ag composites have been extensively studied because added Ag is located in the intergrain region, does not alter T_c and gives rise to low normal state resistivity and improved mechanical properties.

In spite of the fact that Au is often used in physical measurements on superconductors (gold contacts on YBCO exhibit best contact resistances), YBCO–Au composites have been much less investigated, nevertheless, recent works have shown that Au can be incorporated in the YBCO lattice, at $x \leq 0.1$, supposedly at the chain Cu(1) site [4, 5]. The problem of the valence of Au is not yet clear.

In this work, we have attempted to gain insight into the effect of Au on the superconductivity properties of YBCO, in particular on the so called "irreversibility" line (IL).

Among the various magnetic aspects of the behaviour of high T_c superconductors (HTSC) is the existence of an IL in the $H(T)$ diagram. This line separates the region of reversible from irreversible behaviour.

Müller *et al.* [6], then Yeshurun and Malozemoff [7] and Neumann *et al.* [8], found that by increasing applied field, the IL shifted according to

$$H^* = a(1-t)^{\alpha} \quad \text{with } t = T^*/T_c \qquad (1)$$

where $\alpha = 3/2$ (for $H_{\perp}c$) or 4/3 (for $H\|c$) in the case of single crystals and H^* is the irreversible field. The results were explained in terms of a thermally activated flux creep model. Other mechanisms have been suggested to explain IL: either vortex lattice melting [9, 10] or a phase transition from vortex glass to vortex liquid [11]. However, many experimental studies have shown that many HTSC do not follow the behaviour represented by Equation 1: (i) the value α can be different from 3/2 or 4/3; (ii) the law differs according to field range, exponential or power [12–15].

a.c. susceptibility was considered as the most sensitive method for the determination of IL [16, 17]. By this method, the IL is defined as the relation between the temperature T_m (or T_g) of the peak observed in the imaginary part χ'' of the a.c. susceptibility and the a.c. field h or d.c. field H. Very recently, Samarappuli *et al.* [18] and Steel *et al.* [19], by detailed comparison between a.c. susceptibility and resistivity measurements, have suggested that the dissipation peak in χ'' is due to skin size effects and the peak position lines T_m or T_g (h, H) can be interpreted as lines of equal resistivity which approach the d.c. irreversibility line when $\omega \rightarrow 0$. Within the skin effect picture a criterion for the determination of the true IL from a.c. susceptibility measurements can be formulated and it was suggested that the temperature T_{on} where $\chi'' = 0$ rather than the temperature peak indicates irreversible behaviour. Senoussi [39] made the same suggestion in a recent review paper. However, this definition does not yield well-defined values for T^*_{irr}. As already pointed out by Krusin-Elbaum *et al.* [15], under some conditions the maximum in χ'' will occur very near the temperature where nonlinear behaviour is first noted in the I–V curves.

Even if the definition according to which the peak position lines are the IL is not rigorously exact, we believe that the observed influence of Au addition on the temperature peak lines reflects approximately well the situation on the 'irreversibility line'.

* Present address: Laboratoire de Physico-Chimie des Surfaces ENSCP, 11 rue P. et M. Curie 75231 Paris cedex 05, France

0022–2461

2. Experimental procedure

2.1. Sample preparation

The YBCO–Au_x composites were prepared from stoichiometric $YBa_2Cu_3O_7$ and Au powder. $YBa_2Cu_3O_7$ were synthesized by solid state reaction from pure Y_2O_3, $BaCO_3$ and CuO powders. The stoichiometric mixture was ground, pelletized, reacted in air at 950 °C for 24 h and cooled at room temperature. This procedure was done three times. Finally the pellet was oxidized in flowing O_2 at 950 °C for 1 h, then at 500 °C for 4 h and furnace cooled at room temperature.

$YBa_2Cu_3O_7$ was then finely ground and mixed with Au powder in the ratio $(YBCO)_{1-x}Au_x$ ($x \leq 0.3$). The mixture was sintered in flowing O_2 at 950 °C for 17 h, then at 500 °C for 4 h and furnace cooled at room temperature. The specimens were then characterized by X-ray diffraction. In order to avoid the sample size effect on the a.c. susceptibility [20], samples used in these measurements are parallelepiped-shaped bars having approximately the same dimensions.

2.2. Apparatus

a.c. susceptibility measurements were performed with a home made susceptometer described in a previous work [13], using the standard mutual inductance technique, at a frequency of 312 Hz (except for the lowest a.c. field of 0.18 G), for different times and in the absence or presence of a static field H.

The resistivity has been measured with the aid of an a.c. four probe equipment. Prior to the measurements, the contacts made with Ag lacquer were heated under an O_2 atmosphere at 360–400 °C for 2 h and cooled in a furnace at room temperature in order to minimize contact resistances.

The valence states of ions were determined by photoelectron spectroscopy (XPS), the oxygen concentration by the iodometric titration technique.

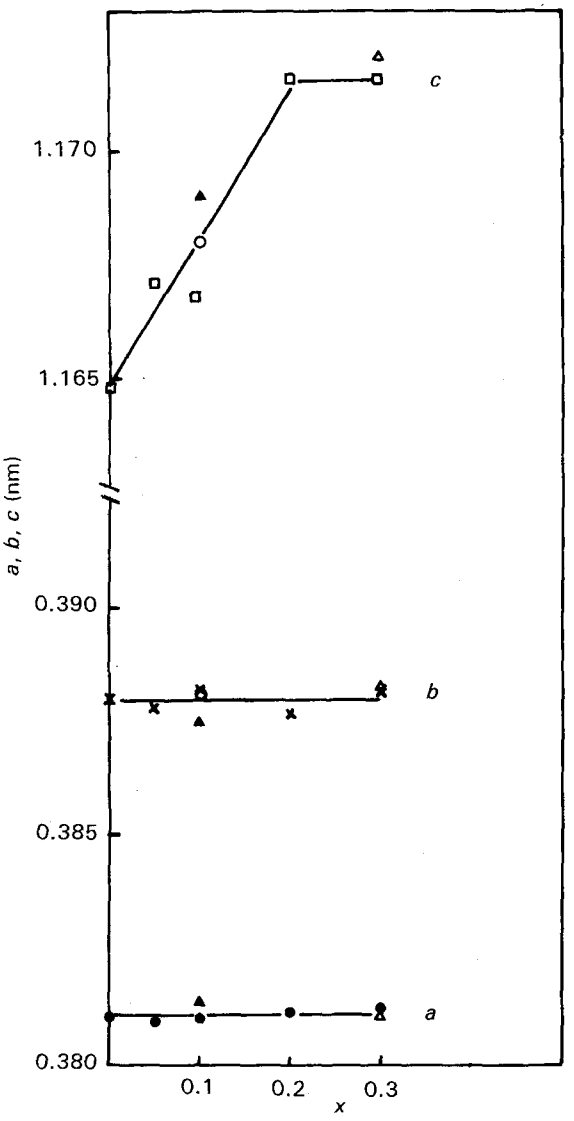

Figure 1 Lattice parameters a, b and c as a function of Au concentration. □, ×, ● $YBa_2Cu_3O_7$–$Au_{0.1}$; ○ $YBa_2Cu_{2.9}O_7Au_{0.1}$; ▲ $Y_{0.9}Au_{0.1}Ba_2Cu_3O_7$; △ $YBa_2Cu_{2.7}Au_{0.3}O_7$.

3. Results and discussion

3.1. Structure of the composites and valence states of Au and Cu

X-ray diffraction measurements have shown that the specimens are single-phased except for $x = 0.2$ and 0.3, where a peak of metallic Au is observed, implying that for these concentrations Au is present in a segregated phase. The structure is orthorhombic for all concentrations. The influence of Au on the lattice parameters is shown in Fig. 1: a and b parameters remain unchanged while c increases up to $x = 0.2$ then becomes constant for $x = 0.3$. As this c expansion is not accompanied by an a or b variation it cannot be attributed to a decrease of oxygen content. Indeed, this latter, determined by chemical titration, is slightly increased by doping ($\delta = 7.00$ for the undoped sample and 7.04 for $x = 0.1$). These results show that Au is incorporated into the $YBa_2Cu_3O_\delta$ structure for $x \leq 0.1$.

The question was about the site occupied by Au. By analysis of X-ray and neutron diffraction results and consideration on the probable valence state of the dopant (Au^{3+}), Hepp *et al.* [21] and Cieplak *et al.* [5] suggested that Au replaces the chain Cu(1). However, our detailed XPS investigation [22] gives evidence that in the YBCO composite the Au valence state is rather close to 1^+ and this value questions the replacement of Cu(1) by Au because of the large difference in ionic radii (Cu^{2+}: 0.073 nm; Au^{1+}: 0.137 nm). Elsewhere, Rudkman and Hepp [23] recently proposed a valence state intermediate between 2 and 3. Furthermore, our XPS results show that the binding energy of the Cu(2p3/2) photoelectron peak in YBCO is not changed by the presence of Au.

For these reasons, we considered replacement at the rare earth site as well as at the Cu ones. We compared $(YBa_2Cu_3O_7)$–$Au_{0.1}$ with $YBa_2Cu_{2.9}Au_{0.1}O_\delta$ and $Y_{0.9}Au_{0.1}Ba_2Cu_3O_\delta$, where the substitution was effectively done on Cu and Y sites, respectively, from the preparation. In contrast to the case of YBCO–$Au_{0.1}$, one can detect traces of second phase in the Cu and Y substituted samples. The Cu substituted sample exhibits similar lattice parameters and supraconducting properties (T_c and χ') (Fig. 2) as the equivalent composite. In contrast, the Y substituted sample shows a slightly larger c parameter, the magnetic transition is

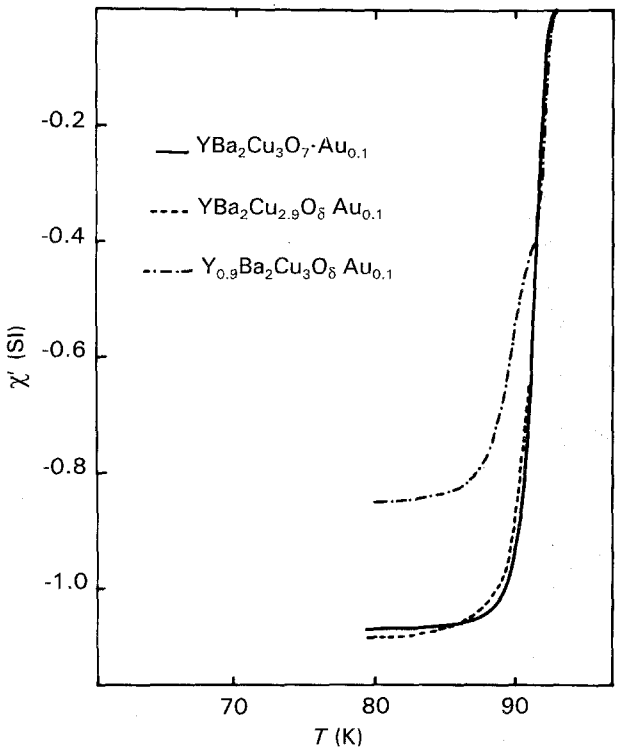

Figure 2 Comparison of the diamagnetic transition of a YBCO–$Au_{0.1}$ composite with that of other substituted samples.

noticeably larger in the low temperature (intergrain) region, whereas in the high temperature (intragrain) region the behaviour is unchanged (same T_c and abrupt onset) and the whole superconducting volume decreases: these observations allow us to suggest that Au does not go to the Y site, $Y_{0.9}Au_{0.1}Ba_2Cu_3O_{6.91}$ behaves in part as grains of YBCO–$Au_{0.1}$ and the lack of Y leads to a more important and less coupled intergrain volume. However, we can suggest that small amounts of Au^{1+} replace Ba^{2+}, since they have a nearly similar radius. Furthermore, this replacement can explain the observed slight increase in the c parameter and enhancement of T_c by the expected increase in hole concentration.

3.2. Resistivity

Resistivity results are shown in Fig. 3, where are plotted normalized resistivity R/R_{295} as a function of temperature for different concentrations x. In normal state, all the specimens are "metallic", meaning that they show a positive temperature coefficient. Above T_c the normalized resistivity can be expressed as

$$R/R_{295} = a + bT$$

The coefficient b is the same for the doped samples, but slightly larger than the value obtained with the undoped one. As shown in Fig. 4, up to $x = 0.1$ the normal state resistivity increases then decreases for $x > 0.1$. At the same time, the T_c defined as the onset temperature of $\rho(T)$ curves increases for $x = 0.05$ and 0.1 and saturates further for $x > 0.1$. One can note the sharpness of the transition for all the doped samples in contrast to the undoped one, which shows a significant tail. These results give fairly good evidence of the

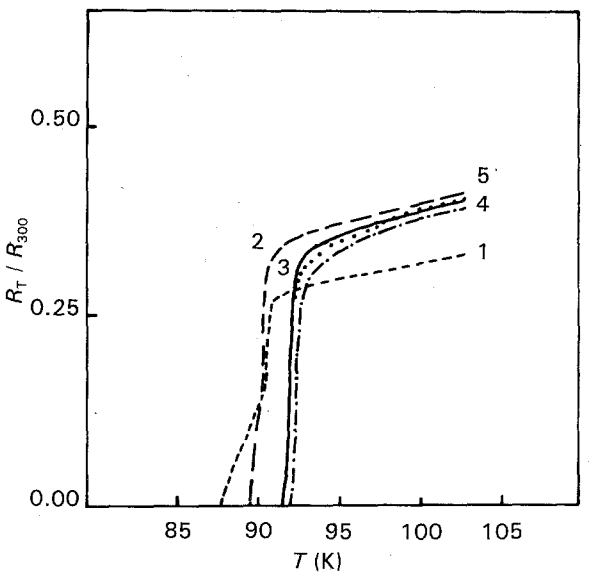

Figure 3 Normalized resistance of YBCO–Au composites as a function of temperature for different Au concentrations. x 1:0; 2:0.05; 3:0.1; 4:0.2; 5:0.3.

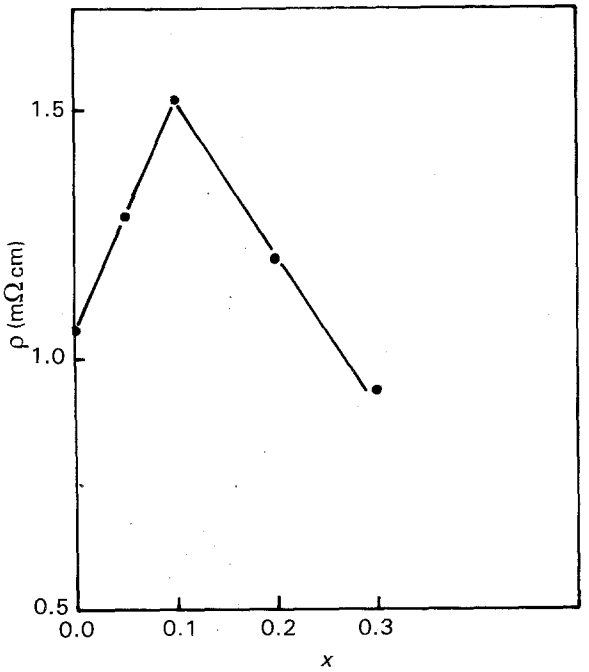

Figure 4 Influence of Au concentration on the room temperature resistivity.

limit of the solubility of Au in grains ($x = 0.1$), in agreement with the literature, and the strengthening of the intergrain coupling by Au doping.

3.3. a.c. susceptibility and peak line

3.3.1. T_c enhancement

Results of a.c. susceptibility measurements for the pure YBCO compound and for doped ones ($x = 0.05$, 0.1, 0.2 and 0.3) are presented in Fig. 5. Superconducting transitions are abrupt in all cases. Au doping tends to sharpen them. T_c is clearly enhanced (about 1.5 K for $x = 0.1$). The onset of $\chi'(T)$ curves is also very abrupt. This may be attributed to a better intragrain coupling and/or to a different microstructure, as can be seen on

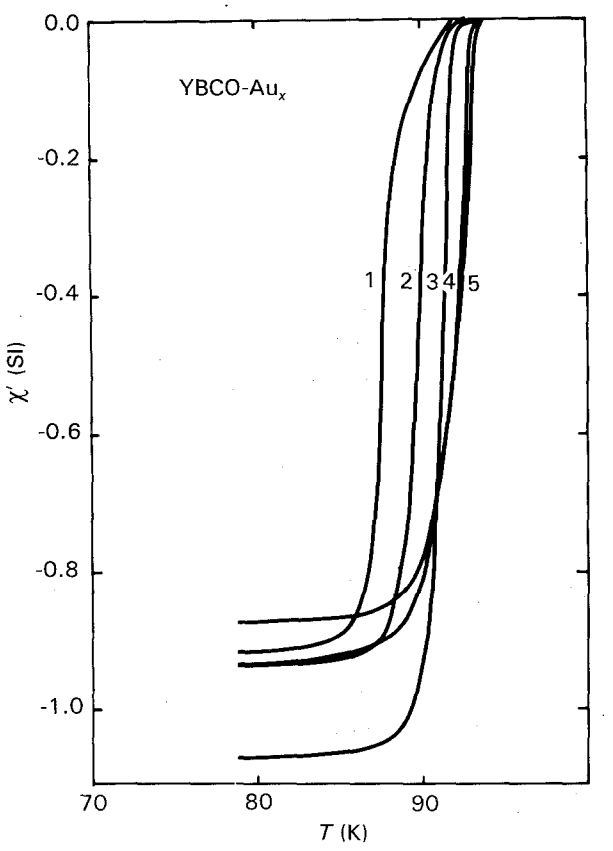

Figure 5 Real part χ' of the a.c. susceptibility as a function of temperature for different x values of YBCO–Au$_x$ composites. x 1:0; 2:0.05; 3:0.1; 4:0.2; 5:0.3.

SEM micrographs (Fig. 6). Pure YBCO shows a typical granular structure with a relatively broad distribution of grain sizes. Gold added to YBCO causes extended grain growth allowing the production of a nearly uniform grain size distribution with relatively large plate-like grains (30–40 μm). Uniformity of grain size should ensure a dense packing of grains and a better coupling of them. The shielding is quasi-complete for all the samples except for $x = 0.1$, where χ' is slightly inferior to -1 (perhaps due to a more important demagnetizing effect or a different density for that sample).

This T_c enhancement may be due to the slight increase in the hole concentration pointed out above. This behaviour is quite different from that of other monovalent dopants such as Li^+ or K^+, which cause an orthorhombic tetragonal transition and decreased superconductivity properties [24].

3.3.2. a.c. field effect

The results are shown in Fig. 7, where are represented the temperature dependence of the real part χ' and the imaginary one χ'' of the pure YBCO compound and doped samples ($x = 0.3$) for different a.c. fields h varying from 0.18 G to 14.4 G. At the lowest h, χ' approaches the value -1, implying complete diamagnetic shielding. With increasing temperature, $\chi'(T)$ exhibits a shoulder which becomes clearly mar-

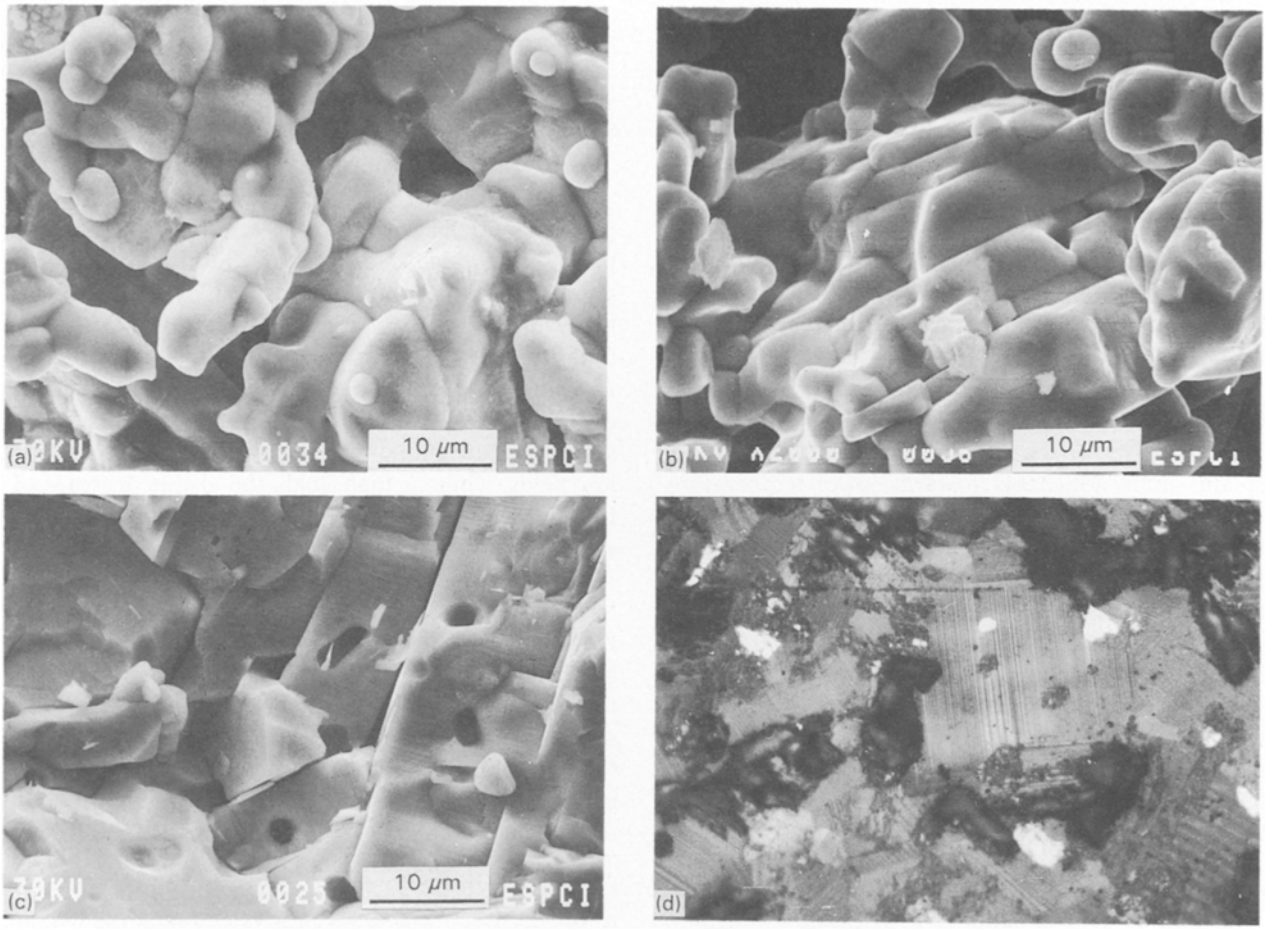

Figure 6 (a, b, c) Scanning electron micrographs of fractured surfaces. (a) undoped sample; (b) YBCO–Au$_{0.05}$; (c) YBCO–Au$_{0.2}$; (d) Optical electron micrograph of YBCO–Au$_{0.2}$ showing Au clusters (bright spots) and large composite crystals.

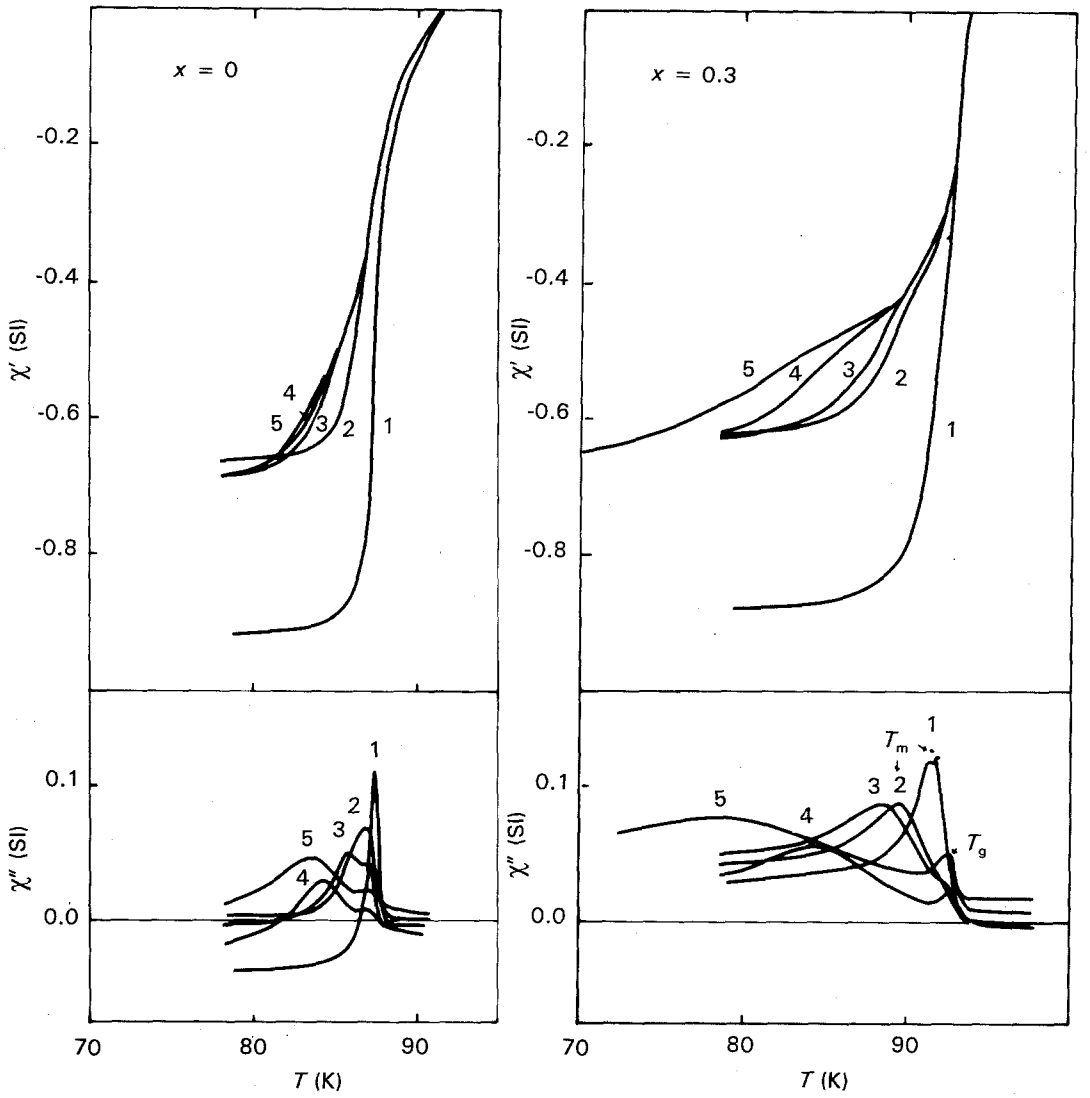

Figure 7 Influence of a.c. field h on the real χ' and imaginary χ'' parts of a.c. susceptibility. h (Gauss) 1:0.18; 2:0.9; 3:1.8; 4:7.2; 5:14.4.

ked at high a.c. fields. As expected, the effect of h is observed only in the low temperature (intergrain) region. Simultaneously, on $\chi''(T)$ curves, a single peak at T_m is observed for low h. At fields higher than H_{c1g} (of grains) a second peak appears at temperature T_g with $T_g > T_m$. These two peaks originate from energy losses in inter and intragrain regions, respectively. With increasing h, the intergrain peak becomes broader and shifts noticeably towards lower temperature, because the intergranular pinning force is rather weak. In contrast, the intragrain peak which appears only at higher fields is only slightly shifted, meaning that in that field range the vortices are strongly pinned in the grain. Qualitatively this kind of variation of χ'' with h has been reported by numerous authors [25–27], but sometimes the high temperature peak T_g is not observed even for a high a.c. field [28, 29], this may be due to many factors: processing procedures inducing different microstructures and more or less hon.ogeneity, sample geometric dimensions, etc.

The influence of a.c. field on T_m (intergrain) and T_g (intragrain) is represented in Fig. 8, where are represented h^* as a function of t; h^* is the a.c. field at which are observed the peaks on $\chi''(T)$ curves, t is the reduced temperature T/T_c where T_c is the onset temperature and T is either T_m or T_g. It can be seen that for $x \leq 0.1$ (which is the limit of solubility of Au in the grains), the curves shift towards higher temperature in the whole h range, revealing a little increase in the intergranular coupling and in the first critical field H_{c1j}, in agreement with resistivity data. For higher Au concentrations ($x = 0.2$ and 0.3) the segregated Au seems to induce a better intergrain coupling only for low fields, while at high fields the visible decrease of the slope dh/dt reflects rather a decrease of this coupling.

In order to analyse for a power law behaviour, we have plotted the data in log–log form (Fig. 9). For all the samples studied the curves are straight lines with, however, a kink for $x = 0.2$ and 0.3, which indicates the separation of the low field region from the high one. The power law is obeyed, but with different slopes (α of Equation 1). In Table I are shown the values of α in low and high field regions.

The main remarks which can be deduced from Table I and Fig. 9 are as follows.

(i) the exponent α is noticeably larger than the values predicted either by the flux creep model (3/2) or the melting transition (2).

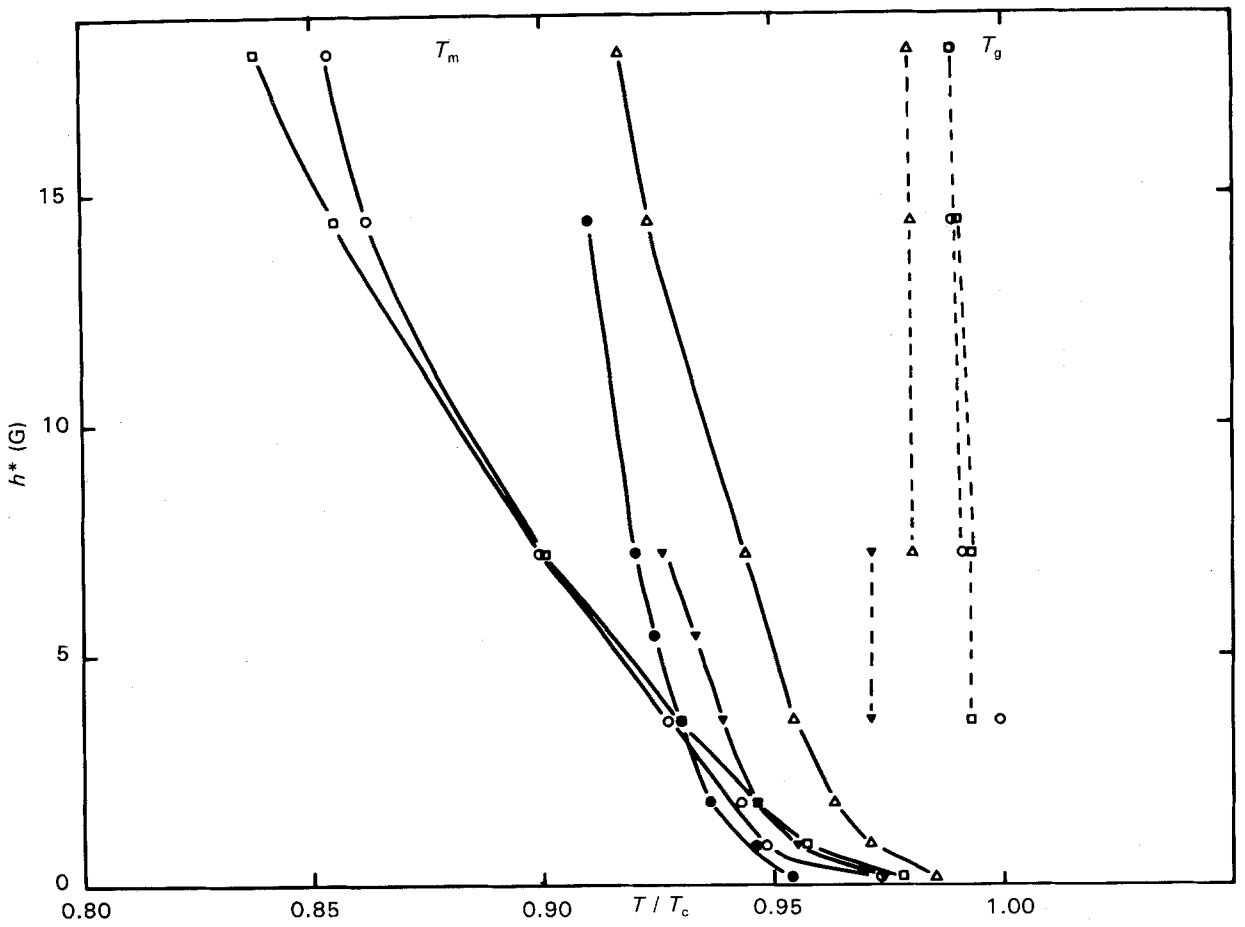

Figure 8 Variation of the normalized temperature T_m/T_c (intergrain) and T_g/T_c (intragrain) of χ'' peaks with a.c. field h. Note the absence of influence of h on T_g. x ●:0; ▼:0.05; △:0.1; ○:0.2; □:0.3.

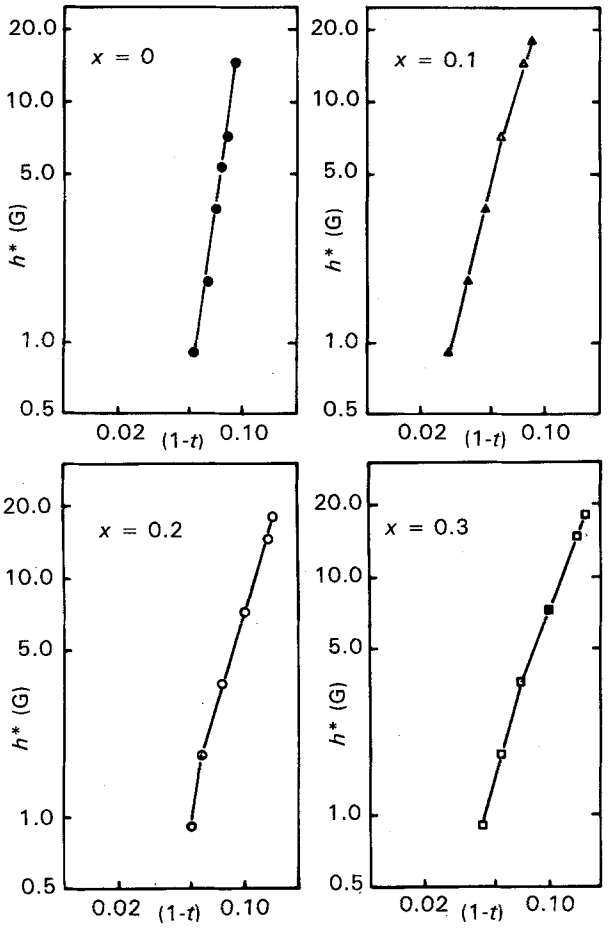

Figure 9 Logarithmic representation of the a.c. field h as a function of $(1 - T_m/T_c)$ for different x-values.

TABLE I Values of α exponent in low and high field regions

x	α Low field	α High field	h^*
0	5.0		
0.05	3.4		
0.1	3.1	2.7	7.2
0.2	6.5	2.3	2.0
0.3	2.8	2.0	2.5

h^* is the field value separating the two regions

(ii) The h^* value indicating the change of the field range depends on x. When $x \geq 0.1$, h^* tends to decrease with increasing x. This behaviour may be attributed to a decrease in the intergrain pinning energy caused by the presence of segregated Au which transforms the SIS junctions into SNS ones.

All these remarks strongly suggest the validity of the model based on flux line pinning; up to the limit of solubility of Au in the grains, Au doping leads to a better intergrain coupling and an increase of the flux pinning energy. For higher Au concentrations this latter parameter tends to decrease. Analogous phenomena were observed by Loegel *et al.* [31] on differently treated samples and by El-Abbar in YBCO–Y_2BaCuO_5 composites [32].

3.3.3. d.c. field effect

As demonstrated above, a small amount of Au is incorporated in the YBCO structure. Hence, it is

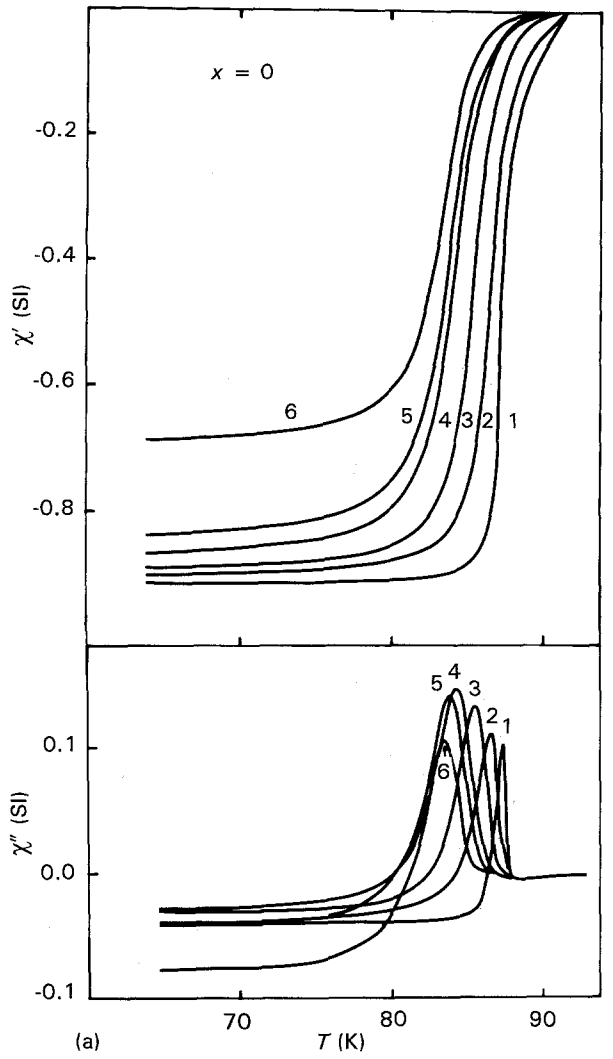

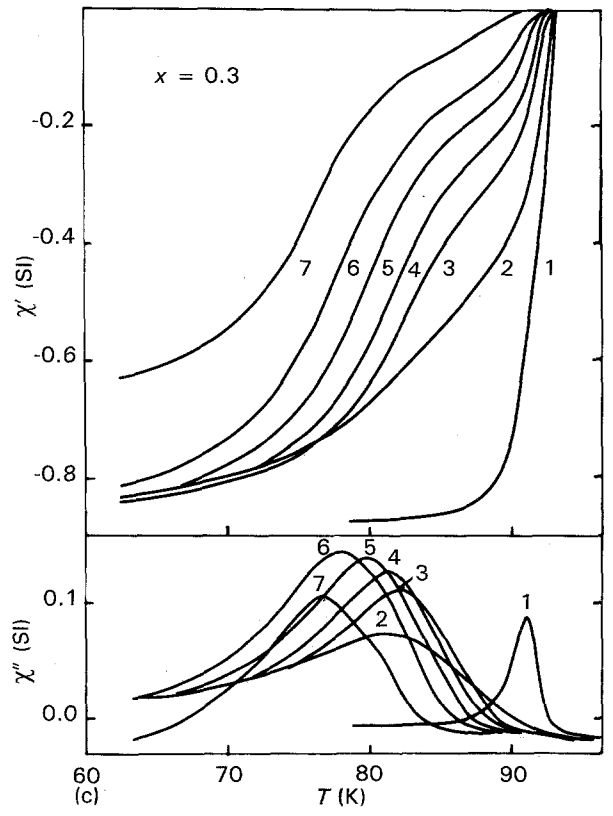

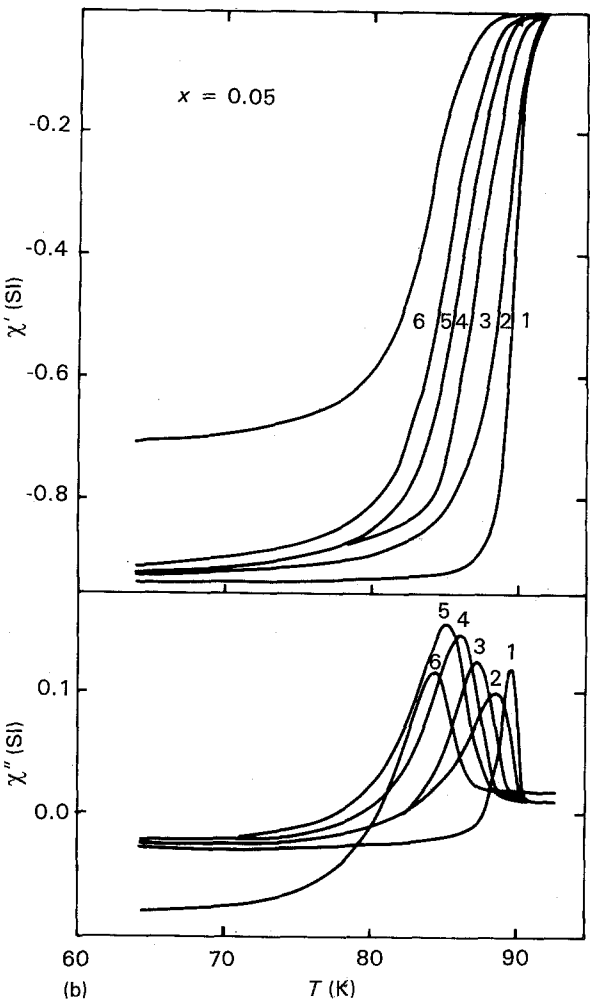

Figure 10 (a) Temperature dependence of the real and imaginary part of the a.c. susceptibility at different static field H of undoped YBCO sample. H (Gauss) 1:0; 2:140; 3:450; 4:2900; 5:4000; 6:5800. (b) Influence of d.c. field on the temperature dependence of the a.c. susceptibility for YBCO–$Au_{0.05}$. H (Gauss) 1:0; 2:140; 3:450; 4:1545; 5:2900; 6:5800. (c) Influence of d.c. field on the temperature dependence of a.c. susceptibility for YBCO–$Au_{0.3}$. H (Gauss) 1:0; 2:140; 3:460; 4:840; 5:1540; 6:2900; 7:5800.

interesting to study the effect of this substitution on the behaviour of the intragrain flux lines. In Fig. 10 we only show the influence of static field H on χ' and χ'' for pure YBCO and $x = 0.05$ and 0.3. With increasing H, T_c is unchanged, χ' (T) becomes broader and broader and the penetration of the field is easier when x increases. χ'' now is due to the motion of vortex lines between and in the grains, since, $H > H_{c1j}$ of weak link junctions. Although we keep in mind that the peak lines do not strictly represent the irreversible line, it is worth analysing the influence of Au doping on the behaviour of these lines. A small shift towards higher temperature is observed only for the slightly doped sample ($x = 0.05$). For $x > 0.1$, the influence of the doping is rather dramatic (Fig. 11). Similarly to intergrain regions, these results can be interpreted as an enhancement of the intragrain coupling and of the first critical field of grains H_{c1g}.

The power law is obeyed for all the samples, however, the exponent α is far from the value predicted by the flux creep theory: α varies from 6 for pure 1 2 3 to approximately 5 for doped compounds. These large values have already been observed in many cases [32] for granular anisotropic superconductors and also for isotropic Chevrel phase superconductors [33].

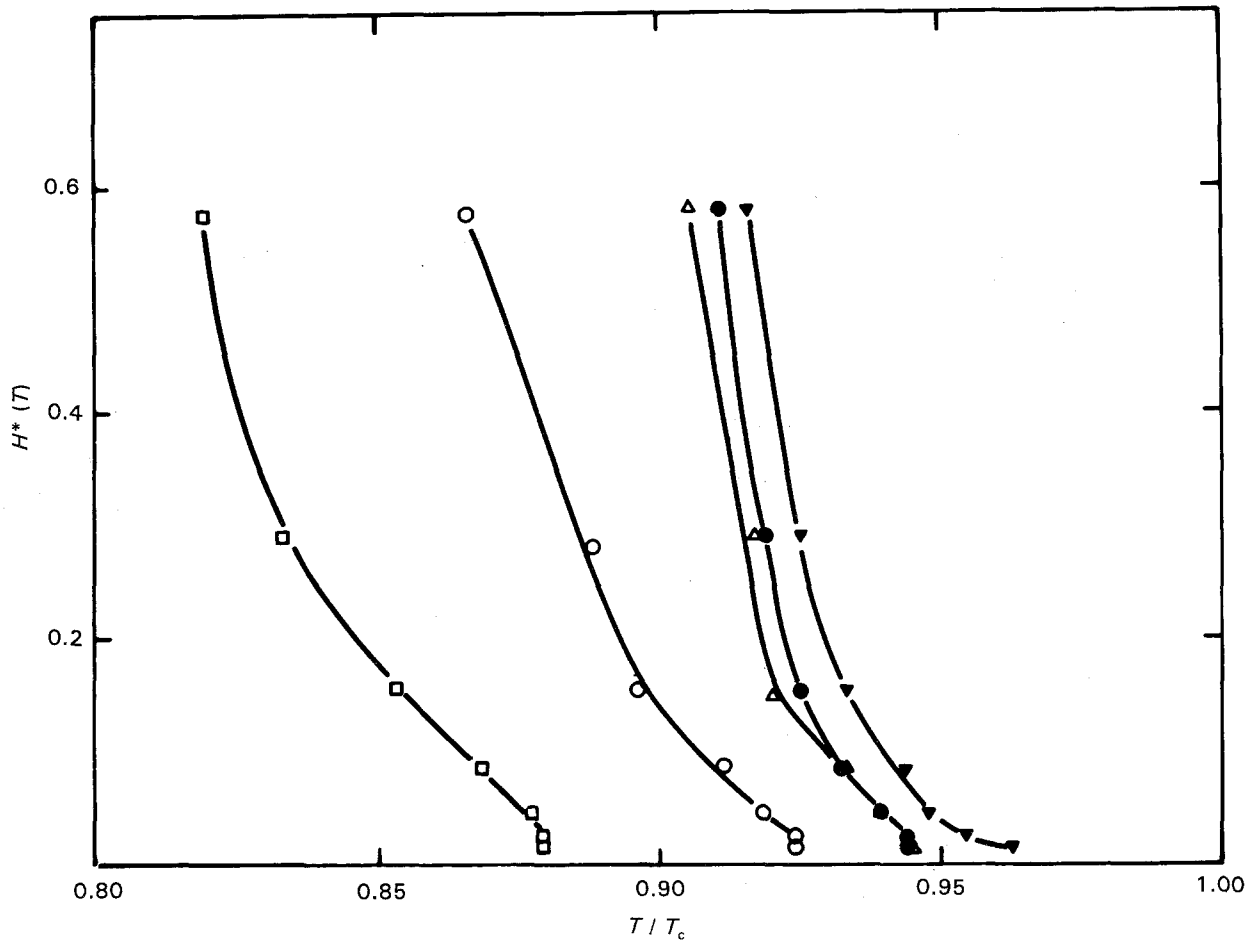

Figure 11 Effect of Au concentration on χ'' peak lines. x ●:0; ▼:0.05; △:0.1; ○:0.2; □:0.3.

4. Conclusions

We have demonstrated that Au can be incorporated in the YBCO lattice up to a concentration 0.1, in the electronic valence state 1^+, hence its replacement at the Cu(1) site becomes questionable due to the large difference in ionic radii of Cu^{2+} and Au^{1+}. For $x > 0.1$, Au is segregated between grains.

The transition temperature is enhanced by 1.5 K. Up to $x = 0.1$ the intergrain and intragrain couplings and first critical fields are improved. We have suggested that this is related to the microstructure of the composite which shows large, uniform sized and oriented grains and to an increase in the hole concentration induced by replacement of small amount of Ba^{2+} by Au^{1+}.

It is interesting to recall the results reported in the literature obtained with YBCO–Ag composites. The influence of added Ag on the microstructure and consequently on the intergrain resistivity and coupling is similar [34–38]. In contrast, Ag does not diffuse into the YBCO structure and does not change the transition temperature. Furthermore, the superconducting properties of Ag composite grains are degraded due to an oxygen deficiency. However, it has been reported that the intergrain critical current density is enhanced.

Finally, it appears that YBCO–Ag and YBCO–Au composites exhibit similar properties, concerning the intergrain regions.

5. Summary

By X-ray diffraction and photoelectron spectroscopy we have demonstrated that Au is incorporated into the YBCO lattice up to a concentration 0.1. An XPS study gave evidence for an electronic valence state Au^{1+}; its replacement on Cu(1) site appears questionable due to the large difference in ionic radii (Cu^{2+}: 0.073 nm; Au^{1+}: 0.137 nm). The so called 'irreversibility lines' determined by a.c. susceptibility measurements are strongly affected by the doping. Up to the limit of solubility of Au in the grains, an improvement in intra and intergrain coupling and first critical fields is observed, showing the beneficial interest of YBCO–Au composites.

References

1. A. V. NARLIKAR, C. V. NARASIMHA RAO and S. K. AGARWAL, in "Studies of high temperature superconductors", edited by A. V. Narlikar, Vol. 1 (New York, Budapest, 1989) p. 341.
2. B. R. WEINBERGER, L. LYNDS, D. M. POTREPKA, D. B. SNOW, C. T. BURILA, H. E. EATON Jr, R. CIPOLLI, Z. TAN and J. I. BUDNICK, *Physica C* **161** (1989) 91.
3. F. H. STREITZ, M. Z. CIEPLAK, GANG XIAO, A. GAVRIN, A. BAKHSHAI and C. L. CHIEN, *Appl. Phys. Lett.* **52** (1988) 927.
4. M. Z. CIEPLAK, GANG XIAO, C. L. CHIEN, J. K. STALICK and J. J. RHYNE, *ibid.* **57** (1990) 934.
5. M. Z. CIEPLAK, GANG XIAO, C. L. CHIEN, A. BAKHSHAI, D. DARTYMOWICZ, W. BRYDEN, J. K. STALIK and J. J. RHYNE, *Phys. Rev. B* **42** (1990) 6200.
6. K. H. MÜLLER, M. TAKASHIGE and J. G. BEDNORZ, *Phys Rev. Lett.* **58** (1987) 1143.
7. Y. YESHURUN and A. P. MALOZEMOFF, *ibid.* **60** (1988) 2202.

8. Ch. NEWMANN, P. ZIEMANN and J. GEERK, *Europhys. Lett.* **10** (1989) 771.
9. P. L. GAMMEL, D. J. BISHOP, G. J. DOLAN, J. R. KWO, C. A. MURRAY, L. F. SCHNEEMEYER and J. V. WASZCZAK, *Phys. Rev. Lett.* **59** (1987) 2592.
10. D. R. NELSON, *ibid.* **60** (1988) 1973.
11. M. P. A. FISHER, *ibid.* **62** (1989) 1415.
12. P. de RANGO, B. GIORDANENGO, R. TOURNIER, A. SULPICE, J. CHAUSSY, G. DEUTSCHER, J. L. GENICON, P. LEJAY, R. RETOUX and B. RAVEAU, *J. Phys.* **50** (1989) 2857.
13. M. NICOLAS, J. NEGRI, J. P. BURGER, *J. Less-Common Metals* **164–165** (1990) 1076.
14. C. NGUYEN, M. NICOLAS, J. NEGRI and J. P. BURGER, *Superconductor Sci. Technol.* **4** (1991) 711.
15. L. KRUSIN-ELBAUM, L. CIVALE, F. HOLTZBERG, A. P. MALOZEMOFF and C. FEILD, *Phys. Rev. Lett.* **67** (1991) 3156.
16. A. M. CAMPBELL, *Cryogenics* **30** (1990) 809.
17. Y. YESHURUN, A. P. MALOZEMOFF, T. K. WORTHINGTON, R. M. YANDROFSKI, L. KRUSIN-ELBAUM, F. HOLTZBERG, T. R. DINGER and G. CHANDRA SEKHAR, *ibid.* **29** (1989) 258.
18. S. SAMARAPPULI, A. SCHILLING, M. A. CHERNIKOV, H. R. OTT and Th. WOLF, *Physica C* **201** (1992) 159.
19. D. G. STEEL and J. M. GRAYBEAL, *Phys. Rev. B* **45** (1992) 12643.
20. V. SKUMRYEV, M. R. KOBLISCHKA and H. KRONMÜLLER, *Physica C* **184** (1991) 332.
21. A. F. HEPP, J. R. GAIER and J. J. POUCH, *J. Solid State Chem.* **74** (1988) 433.
22. C. HINNEN, C. NGUYEN and P. MARCUS, to be published.
23. M. W. RUCKMAN and A. F. HEPP, *J. Appl. Phys.* **70** (1991) 5713.
24. M. NICOLAS, C. NGUYEN VAN HUONG, A. DUBON, G. VETTER and J. CONARD, *J. Physique* **III** (1993) 12.
25. R. B. GOLDFARB, A. F. CLARK, A. I. BRAGINSKI and A. J. PANSON, *Cryogenics* **27** (1987) 475.
26. M. FORSTHUBER, F. LUDWIG and G. HILSCHER, *Physica C* **177** (1991) 401.
27. V. SKUMRYEV, M. R. KOBLISCHKA and H. KRONMÜLLER, *ibid.* **184** (1991) 332.
28. H. MAZAKI, M. TAKANO, R. KANNO and Y. TAKEDA, *Jpn J. Appl. Phys.* **26** (1987) L 780.
29. T. ISHIDA and H. MAZAKI, *ibid.* **26** (1987) L1296.
30. K. H. MULLER, *Physica C* **159** (1989) 717.
31. B. LOEGEL, D. BOLMONT and H. MEHDAOUI, *ibid.* **179** (1991) 15.
32. A. A. EL ABBAR, P. J. KING, K. J. MAXWELL, J. R. OWERS-BRADLEY and W. B. ROYS, *ibid.* **198** (1992) 81.
33. C. ROSSEL, O. PEÑA, H. SCHMITT and M. SERGENT, *ibid.* **181** (1991) 363.
34. B. DWIR, M. AFFRONTE and D. PAVUNA, *ibid.* **162–164** (1989) 351.
35. J. JUNG, M. A. K. MOHAMED, S. C. CHENG and J. P. FRANCK, *Phys. Rev. B* **42** (1990) 6181.
36. B. SOULETIE, M. GUILLOT, P. LEJAY and J. L. THOLENCE, *Solid State Commun.* **78** (1991) 717.
37. D. F. LEE, X. CHAUD and K. SALAMA, *Physica C* **181** (1991) 81.
38. UDAYAN DE, S. NATARAJAN and E. W. SEIBT, *ibid.* **183** (1991) 83.
39. S. SENOUSSI, *J. Physique* **III** (1992) 1041.

Received 13 November 1992
and accepted 19 March 1993